

COMPREHENSIVE LOAD DISTRIBUTION MODEL FOR WOOD TRUSS ROOF ASSEMBLIES

*Kelly LaFave*¹

Graduate Student

and

Rafik Y. Itani

Professor and Chair

Department of Civil and Environmental Engineering
Washington State University
Pullman, WA 99164-2910

(Received November 1990)

ABSTRACT

This study developed and verified a comprehensive structural analysis model to predict the distribution of loads in wood truss roof systems. Experimental testing was performed to provide for model verification and included full-scale tests of individual trusses and a complete roof system.

Nine trusses were individually tested to their design load, then placed in a typically constructed and sheathed assembly for roof system testing. The roof assembly tests consisted of loading individual trusses within the roof using various combinations of concentrated vertical loads. Truss reactions, truss loads, and interior bottom chord deflections were electronically measured. The roof assembly was also tested with two types of gable end truss supports.

The load distributions within the roof assembly were found to remain constant up to and beyond twice the roof's design load. The load distributed through load sharing was found to vary from 60% of the applied load in stiffer trusses to 80% of the applied load in relatively limber trusses. Gable end truss support significantly influenced the load carried by the trusses near the ends of the roof.

By considering the truss members as three-dimensional frame elements with semi-rigid end connections, and by rationally assigning rigidity factors to the connected joints, a model was developed in this study that can accurately predict individual truss stiffness and roof assembly load distributions. Distributions predicted by the model compared closely to those obtained experimentally for both individual truss loadings and for superimposed truss loadings. The model developed does not require experimental connector plate parameters and once fully verified, may prove useful in roof system design procedures.

Keywords: Trusses, load sharing, roofs, composite action, connections.

INTRODUCTION

Metal plate connected wood trusses are the most highly engineered structural components in a light-framed structure and, as such, have demonstrated excellent performance. The benefits of building roofs with metal plate connected trusses include reduced cost, efficient use of materials, better fabrication quality con-

trol, and faster field erection. Examinations of roofs in disaster areas have shown that wood trussed roofs can survive loadings considerably greater than design levels (Gromala and Sharp 1988). While due partly to conservative truss designs, much of the performance of these highly indeterminate systems is due to the redistribution of extreme loads through component interaction, called load sharing.

Load sharing, for the purposes of this study, can be defined as any redistribution of load among the trusses in a roof system due to com-

¹ Present address: Assistant Engineer, Peratrovich, Nottingham and Drage, Inc. 1100 Eastlake Ave. E., Seattle, WA 98109.

ponent interaction. The objective of this study was to develop and verify through comparisons with experimental data, an analytical model that can accurately predict the redistribution of loads within typical wood trussed roof systems due to load sharing. The ability to predict the redistribution of vertical loads is a necessary step in completely understanding roof system performance and is vital to the adoption and implementation of rational design procedures that provide an accurate assessment of roof safety.

REVIEW OF PREVIOUS RESEARCH

Most truss studies are performed either to confirm truss designs or to provide data for truss model verification. In a recent series of studies, a wealth of experimental data was obtained concerning metal plate connected trusses and wood truss roof assemblies. The first part of the comprehensive study was aimed at obtaining connector plated joint properties for use in computer model studies and to study the factors that affect truss joint performance (McCarthy and Wolfe 1987). The modulus of elasticity of the wood members was shown to slightly affect the stiffness of the joint, and the variability of truss plate strength and stiffness was estimated to be about 10–15%.

The second part of the study consisted of conducting full-scale individual tests on 42 wood trusses (Wolfe et al. 1986, 1988). It was observed that truss member stiffness influenced not only truss stiffness, but truss strength and mode of failure as well. It was also reported that the stiffer wood trusses in the study tended to be stronger and to fail at their connections. The limber trusses in the study tended to be weaker and to fail in the truss members themselves. The load-deflection responses of the trusses in the study were observed to be nearly linear up to twice their design load.

To further the study, roof assemblies were constructed using the previously tested trusses. The assemblies were then tested to evaluate the effects of roof configuration and truss stiffness variability on load sharing (Wolfe et al. 1988). All the roof assemblies were found to

exhibit nearly linear load-deflection responses. The load distributions in the roof assemblies, when expressed as percent of applied loads, remained constant up to the first truss failure. It was also shown that the redistribution of loads in a uniformly loaded roof assembly could be approximated by superimposing the load distributions obtained by loading roof trusses individually.

The series of roof assemblies were next computer modeled to predict the redistribution of loads due to load sharing (Cramer and Wolfe 1989; Cramer et al. 1988). The simplified model used in the study represented each truss as simply supported and entirely pin connected. Composite action effects were accounted for by increasing the moments of inertias of the top chords. Mutual constraint effects were included by modeling the roof sheathing as a single continuous beam on each side of the roof. No attempt was made to include connector plate semi-rigidity effects in the model.

The truss reactions and peak deflections predicted by the model were compared to values obtained in roof assembly tests. The simplified model was found to reasonably predict roof assembly load distributions and deflections. The model was particularly accurate in the roof assemblies with extreme variations in truss stiffness. It was concluded from the modeling results that the relatively simple model could closely predict the load distribution, although a more realistic prediction probably could be obtained with a model that accounted for connector plate rigidity and provided a more realistic distribution of roof sheathing stiffness.

It should be noted that very extensive finite element models that accurately predict roof assembly behavior have been developed and reported in the literature (Foschi 1977, 1979). These models require extensive experimental data and are of limited use to the design engineer. There exists a need for a simple model that accounts for connector plate rigidity and distributed sheathing stiffness and that is applicable to a variety of truss types and configurations. To be useful in design, an analytical model must provide an accurate prediction of

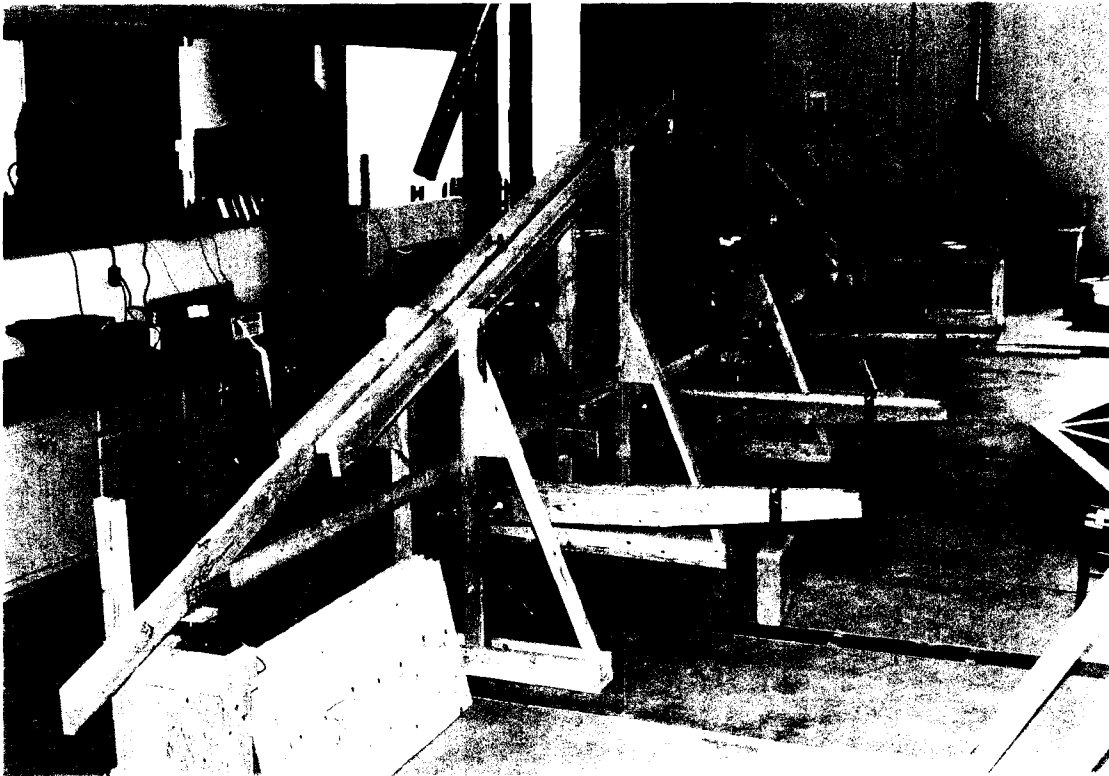


FIG. 1. Individual truss testing in progress.

roof assembly performance, without requiring significant operator time or experimental data.

EXPERIMENTAL PROCEDURE

The trusses used in the full-scale tests were constructed by local truss manufacturers according to the Truss Plate Institute's recommendations and the requirements of the local building code. Truss design was performed for a uniform roof loading of 37 psf (1.8 kPa), for a clear span of 32 ft (9.75 m) and a 2-ft (0.6 m) on center truss spacing. The trusses were fabricated in a Fink truss pattern using visually graded Douglas-fir members and included 2×6 (40 × 140 mm) top chords, 2×4 (40 × 90 mm) bottom chords and 2×4 webs. The trusses were joined using 20 gauge steel plate connectors.

The trusses for the roof assembly were first tested individually to obtain their load deflection responses outside of the roof assembly.

Each truss was tested vertically in a special testing frame that laterally supported the truss and provided for its free vertical displacement and horizontal expansion (see Fig. 1). Various combinations of concentrated vertical loads were applied to the trusses at their top chord panel points. The loads were applied to the trusses in 120-lb increments (0.54 kN) to the truss's design load of 600 lb (2.5 kN) per node. Truss loadings, support reactions, and bottom chord displacements were recorded for each load increment of each load combination.

By defining the stiffness of a truss as the slope of its experimental load-deflection curve, relative stiffness values for the trusses were determined and used to place them in a sequence that led to intensified roof assembly load sharing. Special care was taken during roof construction to ensure that the trusses were placed at their proper spacing, that the recommended gaps between sheathing panels were main-

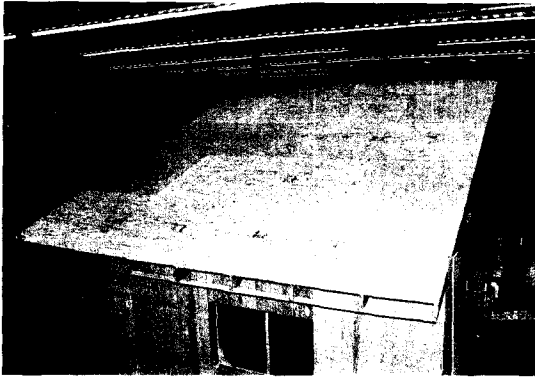


FIG. 2. Roof assembly completely sheathed and ready for testing.

tained, and that the nails were accurately driven at the correct intervals. The roof assembly is shown in Fig. 2.

The roof assembly was completely isolated on load cells. Truss reactions and applied loads were directly measured with load cells placed under each truss and in-line on each of the loading mechanisms. The load cells supporting one end of the roof contained rollers that allowed the roof to deflect horizontally as the trusses were loaded. Roof assembly deflections were measured with linear variable differential transformers (LVDTs), mounted along the bottom chords of the trusses. Load cell and LVDT data were recorded with a programmable datalogger and were read immediately upon loading and again after the loads had been maintained on the roof assembly for 5 min.

The roof assembly was tested with two types of gable end truss support configurations. In the first test, the end trusses were supported on load cells only at their ends, just as the interior trusses. During the second test, the end trusses were supported on wood blocks equally spaced along their bottom chords to simulate the extra stiffness of a sheathed gable end truss.

EXPERIMENTAL RESULTS

By defining the load carried by a given truss as the sum of its two measured reactions, the load distribution in the roof assembly at any truss loading can be calculated and plotted for

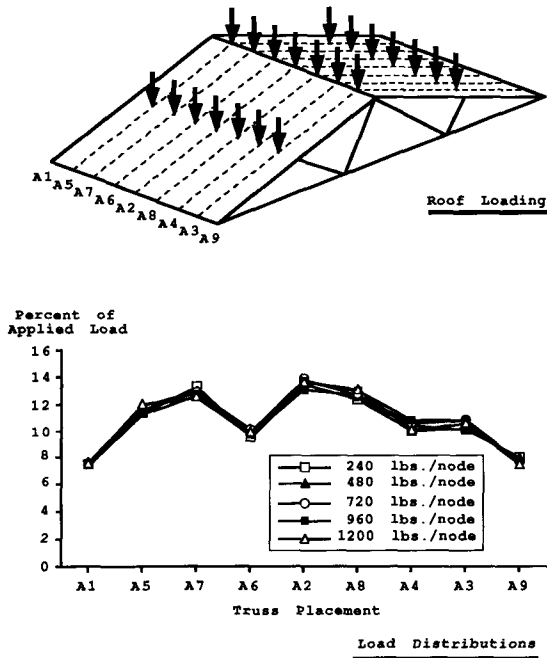


FIG. 3. Experimental superimposed distributions at roof loadings up to twice truss design load.

comparison with model predictions. The superimposed individual truss loadings for up to twice the design load of the roof are plotted in Fig. 3. As can be observed in the figure, the distribution of load throughout the roof remained nearly constant throughout the load range used in the roof test. This supports the assumption that a linear model will be adequate in predicting the load distribution in the roof assembly at load levels up to twice its design load.

The influence of sheathed gable end trusses on the load distribution within the roof assembly is presented in Fig. 4. The propped gable end trusses attracted a large portion of load from their two adjacent trusses but had little influence on the load carried by the trusses farther than two truss spans away from the gable end trusses.

ANALYTICAL PROCEDURE

The complete roof assembly, consisting of trusses equally spaced and sheathed with plywood, was modeled entirely with three-dimensional frame elements. Three-dimension-

al modeling is necessary for the roof assembly because the roof trusses deflect both vertically and laterally when loaded. The local degrees of freedom associated with three-dimensional frame elements and their transformations to global degrees of freedom are well covered in several textbooks on matrix structural analysis (Wang 1986) and will not be discussed here.

The force-displacement equation for a three dimensional frame element with the 12 degrees of freedom (see Fig. 5) can be expressed with respect to the element's local axes with the force vector on the left and the stiffness matrix and displacement vector on the right side of the equation (see Eq. (1), below). The force vector consists of the forces and moments required for static equilibrium of the element when its ends undergo the displacements and rotations of the displacement vector. The stiffness matrix contains the relationships between displacement of the ends of an element and its equilibrium forces. Each column of the stiffness matrix relates the forces induced in the frame element by a unit displacement in the direction of a degree of freedom.

To account for the additional flexibility of the plated truss joints, the stiffness matrix associated with a three-dimensional, rigidly connected frame element was modified to incorporate semi-rigid joints. The modified coefficients of the stiffness matrix can be expressed as:

$$K1 = \frac{3AE}{L \left(\frac{1}{PA_i} + \frac{1}{PA_j} + 1 \right)} \tag{2}$$

$$K2 = \frac{3GI_x}{L \left(\frac{1}{T_i} + \frac{1}{T_j} + 1 \right)} \tag{3}$$

$$K3 = \frac{12EI_y P_i}{L(4 - P_i P_j)} \tag{4}$$

$$K4 = \frac{6EI_y P_i P_j}{L(4 - P_i P_j)} \tag{5}$$

$$K5 = \frac{12EI_y P_j}{L(4 - P_i P_j)} \tag{6}$$

$$K6 = \frac{12EI_z S_i}{L(4 - S_i S_j)} \tag{7}$$

$$K7 = \frac{6EI_z S_i S_j}{L(4 - S_i S_j)} \tag{8}$$

$$K8 = \frac{12EI_z S_j}{L(4 - S_i S_j)} \tag{9}$$

$$K9 = (K3 + K4)/L \tag{10}$$

$$K10 = (K4 + K5)/L \tag{11}$$

$$K11 = (K6 + K7)/L \tag{12}$$

$$K12 = (K7 + K8)/L \tag{13}$$

$$K13 = (K3 + 2 \cdot K4 + K5)/L^2 \tag{14}$$

$$K14 = (K6 + 2 \cdot K7 + K8)/L^2 \tag{15}$$

$$\begin{pmatrix} M_{xi} \\ M_{yi} \\ M_{zi} \\ F_{xi} \\ F_{yi} \\ F_{zi} \\ M_{xj} \\ M_{yj} \\ M_{zj} \\ F_{xj} \\ F_{yj} \\ F_{zj} \end{pmatrix} = \begin{bmatrix} K2 & 0 & 0 & 0 & 0 & 0 & -K2 & 0 & 0 & 0 & 0 & 0 \\ 0 & K3 & 0 & 0 & 0 & -K9 & 0 & K4 & 0 & 0 & 0 & K9 \\ 0 & 0 & K6 & 0 & K11 & 0 & 0 & 0 & K7 & 0 & -K11 & 0 \\ 0 & 0 & 0 & K1 & 0 & 0 & 0 & 0 & 0 & -K1 & 0 & 0 \\ 0 & 0 & K11 & 0 & K14 & 0 & 0 & 0 & K12 & 0 & -K14 & 0 \\ 0 & -K9 & 0 & 0 & 0 & K13 & 0 & -K10 & 0 & 0 & 0 & -K13 \\ -K2 & 0 & 0 & 0 & 0 & 0 & K2 & 0 & 0 & 0 & 0 & 0 \\ 0 & K4 & 0 & 0 & 0 & -K10 & 0 & K5 & 0 & 0 & 0 & K10 \\ 0 & 0 & K7 & 0 & K12 & 0 & 0 & 0 & K8 & 0 & -K12 & 0 \\ 0 & 0 & 0 & -K1 & 0 & 0 & 0 & 0 & 0 & K1 & 0 & 0 \\ 0 & 0 & -K11 & 0 & -K14 & 0 & 0 & 0 & -K12 & 0 & K14 & 0 \\ 0 & K9 & 0 & 0 & 0 & -K13 & 0 & K10 & 0 & 0 & 0 & K13 \end{bmatrix} \begin{pmatrix} \theta_{xi} \\ \theta_{yi} \\ \theta_{zi} \\ \delta_{xi} \\ \delta_{yi} \\ \delta_{zi} \\ \theta_{xj} \\ \theta_{yj} \\ \theta_{zj} \\ \delta_{xj} \\ \delta_{yj} \\ \delta_{zj} \end{pmatrix} \tag{1}$$

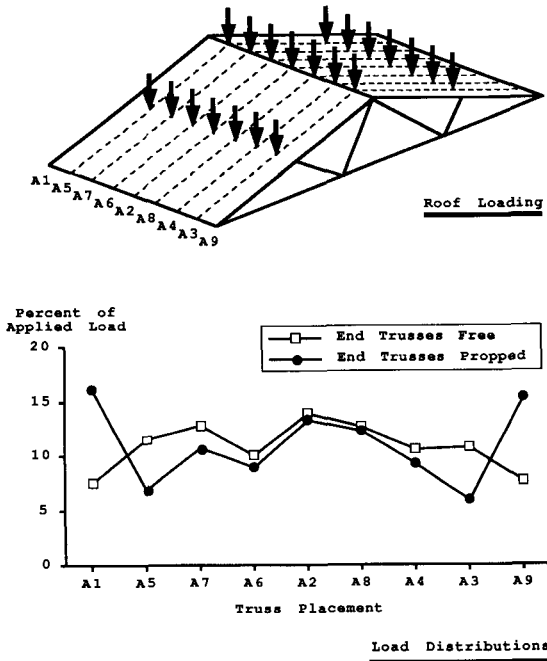


FIG. 4. The effects of propped gable end trusses on superimposed load distribution.

I_x , I_y and I_z are the frame element's moments of inertia with respect to the local X, Y, and Z axes, respectively. PA_i and PA_j are the axial fixity factors at the initial and terminal ends of the element and T_i and T_j are the initial and terminal end torsional fixity factors. P_i , P_j , S_i , and S_j are the rotational fixity factors of the initial and terminal ends of the beam with respect to bending moments about the local Y and Z axes.

In the derivation of the stiffness matrix coefficients (LaFave 1990), joint semi-rigidity was expressed with joint fixity factors. The fixity factors relate the fixity of a semi-rigid joint to the fixity of a completely rigid joint. By definition, a completely fixed joint has a joint fixity factor of 100%. To apply the stiffness matrix derived for frame members with semi-rigid joints to metal plate connected trusses, the fixity factors of truss plated joints for each degree of freedom must be computed. In this study, a rational method of calculating fixity factors by considering the effective volume of wood directly in contact with the nails of a connector plate was developed.

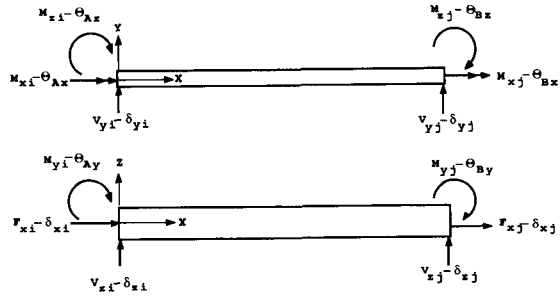


FIG. 5. Degrees of freedom and local coordinate axes for a three-dimensional frame element.

Rotational fixity factors were estimated using the ratio of connector plate to truss member moment of inertia. The connector plate moment of inertia was calculated using the volume of wood in contact with the nails of the connector plate. By defining the area of plate nail contact as the width of the connector plate times its nail penetration depth, the connector plate moment of inertia can be calculated in the normal way. For example, the rotational fixity factor about the strong axis of a joint can be written as

$$P = \frac{P_n w_p^3}{6I_y} \tag{16}$$

and the rotational fixity about the weak axis of a joint can be expressed as

$$S = \frac{w_p(W^3 - 2P_n^3)}{12I_z} \tag{17}$$

where P_n is the connector plate nail penetration, w_p is the width of the plate, and W is the width of the frame element. I_y and I_z are the moments of inertia of the frame element about its Y and Z axes, respectively. The torsional fixity factor can be calculated similarly.

The uniaxial fixity factor was estimated using the ratio of the effective cross-sectional areas of the plate connector and the frame member. As with the moment of inertias, the effective cross-sectional area of the plated joint was calculated by considering the wood directly confined by the nails of the connector plate and can be expressed as

$$PA = \frac{2P_n w_p}{A} \tag{18}$$

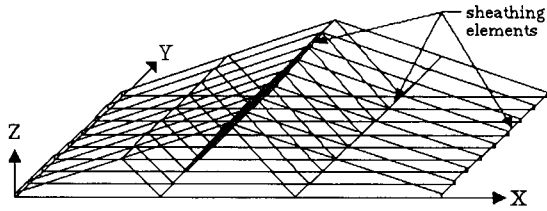


FIG. 6. Roof assembly model 1 analog using 3-D frame elements.

where P_n and w_p have been previously defined and A is the cross-sectional area of the frame member being connected. Shear deformations were not included in the derivation of the model, so fixities for the two shear directions are not required in the analysis.

Truss chord continuity is accounted for in the analysis model by assigning rotational and axial fixity factors of 100% to the ends of members continuous through a joint. Hinges or true pin connections can be included in an analysis by assigning rotational fixity factors equal to zero.

Two different frame element models were used to simulate the experimental roof assembly. The first model (Fig. 6) consisted of 9 trusses (10 nodes and 14 members each) connected with 40 elements to simulate the roof sheathing. The roof sheathing stiffness was lumped in five rows of elements that connected the top chord panel points of the trusses. The stiffness assigned to a particular element was proportional to the tributary width of the sheathing that the element represented.

The second model (Fig. 7) represented the roof assembly with 9 trusses (13 nodes and 17 members each) and 72 elements to simulate the roof sheathing. In this analog, the roof sheathing stiffness was distributed within the

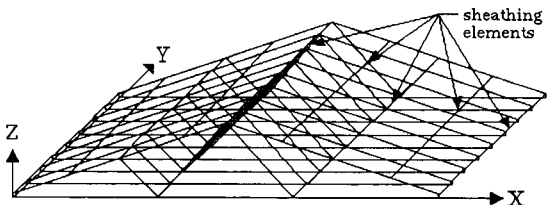


FIG. 7. Roof assembly model 2 analog using 3-D frame elements.

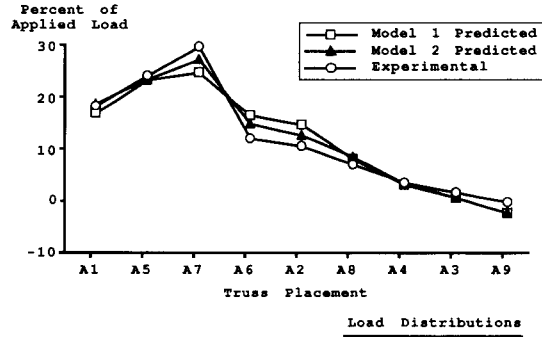
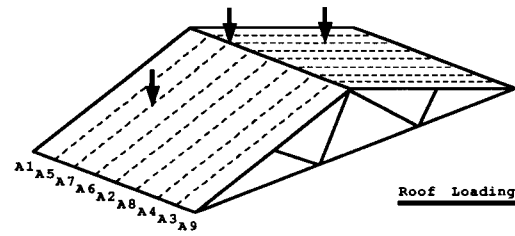


FIG. 8. Distributions predicted for truss A7 individually loaded.

plane of the roof and every element representing sheathing had the stiffness properties of a standard width sheet of plywood.

In both roof models, the stiffness properties of the sheathing elements were transformed to account for their orientation along the slope of the roof and the moments of inertia of the truss top chords were increased to account for composite action effects.

ANALYTICAL RESULTS

The ability of the two roof models to predict load distributions in the roof assembly is shown by plotting the model results versus the distributions obtained in the roof test. The percent of load carried by a truss is the sum of its two reactions divided by the total applied load.

In Fig. 8, the distributions predicted by the two models are shown with the actual distribution obtained by individually loading truss A7 at all three of its top chord nodes. In Fig. 9, the predicted and experimental distributions are shown for truss A4 individually loaded at all three of its top node points and in Fig. 10, the predicted and experimental dis-

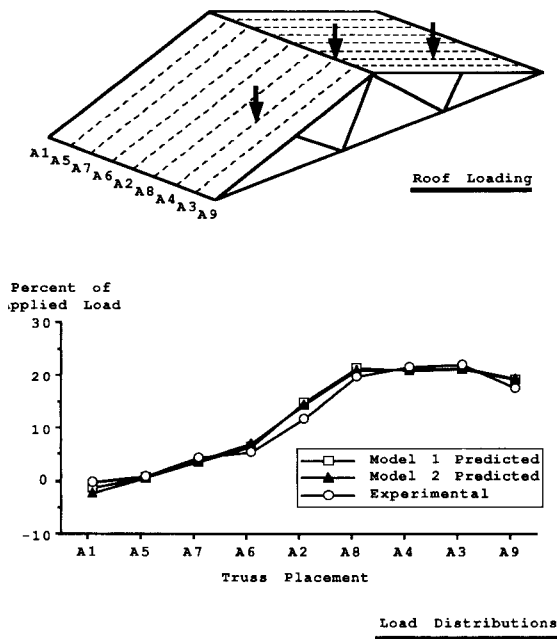


FIG. 9. Distributions predicted for truss A4 individually loaded.

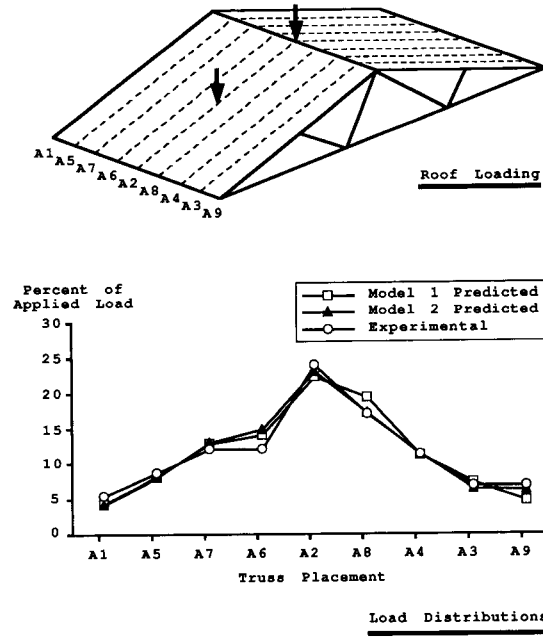


FIG. 10. Distributions predicted for truss A2 loaded at its center and left nodes.

tributions for truss A2 left side loaded. The predictions of both roof assembly models closely agree with the distributions obtained experimentally.

The predicted load distributions appear smoother than the experimental distributions. The model tends to distribute loads to trusses evenly in situations where the experimental curves show large differences in loads carried by adjacent trusses. This discrepancy may be caused by lumping sheathing properties at truss nodes. The distributions predicted by the second model 2 give a slightly better fit to the experimental distributions, possibly because the sheathing elements are better distributed along the roof. It also may be possible that, with further refinement of the elements representing the sheathing, closer predictions can be obtained.

The distributions predicted by the roof assembly models for all interior trusses loaded are presented with the superimposed experimental distribution in Fig. 11. Excellent agreement has been obtained between the predicted

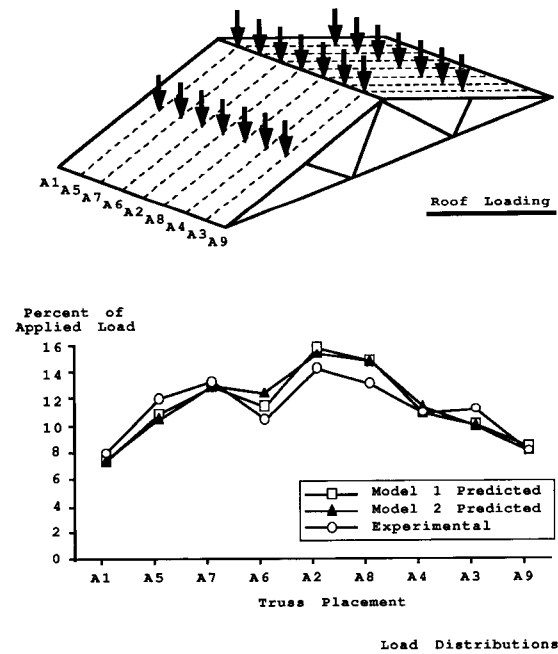


FIG. 11. Distributions predicted for all interior trusses loaded.

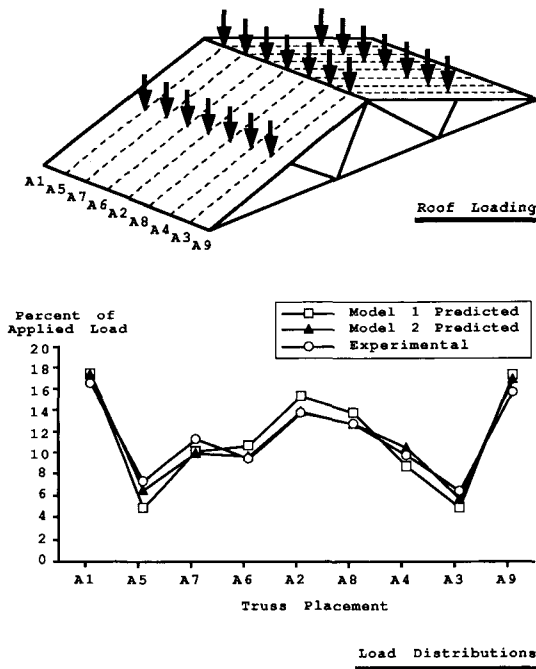


FIG. 12. Distributions predicted for all interior trusses loaded and gable end trusses propped.

and experimental distributions. Both of the predicted load distributions fit the actual distribution to within 2% of the applied load.

In Fig. 12, the model predicted and experimental load distributions for the roof assembly with propped gable end trusses are shown. The distributions predicted by both models again closely fit the experimental. This demonstrates the ability of the analytical procedure to predict the load distribution in varied roof assembly configurations and supports the model's applicability for use in roof assembly analysis.

CONCLUSIONS

The primary conclusion drawn is that the model developed in this study can accurately predict the distributions of loads in the tested roof assembly. By modeling the roof assembly using three-dimensional frame elements with semi-rigid joints, a better prediction of roof assembly behavior was obtained over the predictions of simpler models reported in the literature.

Because the modeling approach yielded good predictions of load distributions for all loading combinations and for both types of gable end truss support, it appears to be applicable to a variety of roof configurations and loadings.

Once the method of modeling wood truss roof assemblies, as presented here, is fully validated through additional testing, it can be used to help quantify the effects of load sharing and to help develop roof design procedures that incorporate the roof strength and reliability benefits of load sharing. Because the method of using semi-rigid joints to model truss plate connections provides a realistic prediction of truss displacements and member forces, it also can be useful in the design of individual trusses.

ACKNOWLEDGMENTS

This research was conducted as part of NSF Grant No. MSM8613509. Opinions and findings expressed in this paper are those of the authors and do not reflect the views of the sponsor.

REFERENCES

- CRAMER, S. M., AND R. W. WOLFE. 1989. Load distribution model for light-frame wood roof assemblies. *J. Struct. Eng., ASCE*. 115(10):2603-2616.
- , ———, AND A. PEYROT. 1988. Modeling roof systems for reliability analysis. Pages 143-150, vol. 1, in R. Y. Itani, ed. *Proc. of the 1988 International Conference on Timber Engineering*. Forest Products Research Society, Madison, WI.
- FOSCHI, R. O. 1977. Analysis of wood diaphragms and trusses. Part II. Truss plate connections. *Can. J. Civ. Eng.* 4(3):354-360.
- . 1979. Truss plate modeling in the analysis of trusses. Pages 88-97 in *Proc. of Metal Plate Wood Truss Conference*. Forest Products Research Society, Madison, WI.
- GROMALA, D. S., AND D. J. SHARP. 1988. Concepts of wood structural system performance. Pages 136-142, vol. 1, in R. Y. Itani, ed. *Proc. of the 1988 International Conference on Timber Engineering*. Forest Products Research Society, Madison, WI.
- LAFAVE, K. D. 1990. Experimental and analytical study of load sharing in wood truss roof systems. Unpublished M.S. thesis, Washington State University, Pullman, WA.
- MCCARTHY, M., AND R. W. WOLFE. 1987. Assessment of truss plate performance model applied to southern

- pine truss joints. USDA Research Paper FPL-RP-483, Forest Prod. Lab., Madison, WI.
- WANG, C. K. 1986. Structural analysis on microcomputers. Macmillan, New York, NY.
- WOLFE, R. W., T. LABISSONIERE, AND S. M. CRAMER. 1988. Performance tests of light-frame roof assemblies. Pages 3-11, vol. 2, *in* R. Y. Itani, ed. Proc. of the 1988 International Conference on Timber Engineering. Forest Products Research Society, Madison, WI.
- , D. H. PERCIVAL, AND R. C. MOODY. 1986. Strength and stiffness of light-framed sloped trusses. USDA Research Paper FPL 471. Forest Prod. Lab., Madison, WI.